



Particulate matters emitted from maize straw burning for winter heating in rural areas in Guanzhong Plain, China: Current emission and future reduction



Jian Sun^{a,b}, Zhenxing Shen^{a,b,*}, Junji Cao^b, Leiming Zhang^c, Tingting Wu^a, Qian Zhang^a, Xiuli Yin^d, Yali Lei^a, Yu Huang^b, R-J Huang^b, Suixin Liu^b, Yongming Han^b, Hongmei Xu^a, Chunli Zheng^a, Pingping Liu^a

^a Department of Environmental Sciences and Engineering, Xi'an Jiaotong University, Xi'an 710049, China

^b Key Lab of Aerosol Chemistry & Physics, Institute of Earth Environment, Chinese Academy of Sciences, Xi'an 710049, China

^c Air Quality Research Division, Science and Technology Branch, Environment and Climate Change Canada, Toronto, Canada

^d Guangzhou Institute of Energy Conversion, Chinese Academy of Sciences, 510640, China

ARTICLE INFO

Article history:

Received 28 July 2016

Received in revised form 4 October 2016

Accepted 10 October 2016

Available online 11 October 2016

Keywords:

Residential heating

Maize straw

Particulate matter

Emission factors

ABSTRACT

Maize straw smoldering in "Heated Kang" is the traditional way for heating in winter in rural areas of Guanzhong Plain. This smolder procedure produced large quantities of pollutants and got more and more concern from both public and researchers. In this study, on-site measurements of straw smoldering in a residence with a Chinese 'Heated Kang' (Scenario 1) were done to determine the emissions factors (EFs) for pollutants. Moreover, EFs of pollutants from an advanced stove fired with maize straw (Scenario 2) and maize-straw pellet (Scenario 3) had been conducted in a laboratory to find the new measure to reduce the pollution emissions. The results showed that the EFs of PM_{2.5} for three scenarios were $38.26 \pm 13.94 \text{ g} \cdot \text{kg}^{-1}$, $17.50 \pm 8.29 \text{ g} \cdot \text{kg}^{-1}$ and $2.95 \pm 0.71 \text{ g} \cdot \text{kg}^{-1}$, respectively. Comparing EFs of pollutants from 3 scenarios indicates that both briquetting of straw and advanced stove with air distribution system could efficiently reduce pollutants emission especially for Scenario 3. In detail, EFs of PM_{2.5}, OC, EC and water soluble ions all have over 90% reduction between Scenarios 1 and 3. All particle-size distributions were unimodal, and all peaked in particle sizes $< 0.47 \mu\text{m}$. The EFs for K⁺ and Cl⁻ were the highest of cations and anions for the majority of size groups. Converting to pellets and advanced stoves for residential heating could reduce PM_{2.5} emission from 48.3 Gg to 3.59 Gg, OC from 19.0 Gg to 0.91 Gg, EC from 1.7 Gg to 0.17 Gg and over 90% reduction on total water soluble ions in the whole region. A box model simulation for the Guanzhong Plain indicated that this conversion would lead to a 7.7% reduction in PM_{2.5} (from 130 to 120 $\mu\text{g} \cdot \text{m}^{-3}$) in normal conditions and a 14.2% reduction (from 350 to 300 $\mu\text{g} \cdot \text{m}^{-3}$) in hazy conditions. The results highlighted that the straw pellets burning in advanced stove can effectively reduce pollutants emitted and improve the energy use efficiency in comparison with maize straw smoldering in "Heated Kang". The study supplies an effective measure to reduce the rural biomass burning emission, and this method can be used in not only Guanzhong Plain but also other undeveloped areas in the future.

© 2016 Elsevier B.V. All rights reserved.

1. Introduction

Crop residues are the fourth largest energy resources worldwide after coal, oil, and natural gas. About half of the world's population uses crop residues for domestic heating and cooking, especially in rural areas of developing countries (Cao et al., 2008; Zhang et al., 2011; Shen et al., 2012). In China, it has been estimated that 288 million tons of agricultural biomass were burned in 2000 by rural households for cooking and heating, and that amount accounted for

57% of the total rural household energy use (PRCMA, 2001; PRCDITS, 2005). Unfortunately, biofuel combustion is typically carried out in small household stoves under poor combustion conditions and without any emission controls, which produces a large amount of pollutant emissions (Li et al., 2007; Shen et al., 2011a). Biomass burning is the largest source of primary fine carbonaceous particles and the second largest source of trace gases for the global atmosphere (Andreae and Merlet, 2001; Bond et al., 2004; Guenther et al., 2006). In 2007, the global PM_{2.5} (PM with a diameter $< 2.5 \mu\text{m}$) emissions were 40.0 Tg·year⁻¹, of which 27.0 Tg·year⁻¹ was from biomass burning sources (Huang et al., 2014a, b). Emissions from crop residue burning are spatially and temporally heterogeneous, and the emission factors (EFs) measured for some major pollutant species have varied over several orders-of-magnitude. Large variations in EFs have caused large uncertainties in

* Corresponding author at: Department of Environmental Sciences and Engineering, Xi'an Jiaotong University, Xi'an 710049, China.
E-mail address: zxshen@mail.xjtu.edu.cn (Z. Shen).

emission inventories from biomass sources (Streets et al., 2003; Bond et al., 2004; Shen et al., 2010; Wang et al., 2015).

Particles emitted from biomass burning are predominantly carbonaceous materials, including both organic carbon (OC) and elemental carbon (EC), which have major direct and indirect climate impacts (Rosenfeld, 1999; Menon et al., 2002). OC scatters solar radiation and cool the atmosphere while EC absorbs solar radiation and heats the atmosphere. In fact, EC is the third largest contributor to global warming, only after CO₂ and CH₄ (Menon et al., 2002; Sato et al., 2003; Gustafsson et al., 2009). Biomass burning also produces water-soluble inorganic ions (e.g., potassium, sodium, chloride, and calcium) and hygroscopic organic compounds since these compounds are crop residues, and once released into the atmosphere they can act as cloud condensation nuclei (CCN) and likely reduce the net flux of solar radiation to the Earth's surface (Rose et al., 2010; Latham et al., 2013). In addition to the production of aerosols, biomass burning also emits large amounts of gaseous pollutants, including CO₂, CO, NO_x, and polycyclic aromatic hydrocarbons (Zhang et al., 2015).

The Guanzhong Plain area is ~36,000 km², with a population about 23.92 millions. Guanzhong Plain where atmospheric dispersion is usually weak due to the unique features of its topography, that's surrounded by Qinling Mountains to the south and the Loess Plateau to the north (As shown in Fig. S1). The traditional way for residential heating in winter in rural areas is burning maize straw in "Heated Kang". Maize straw smoldering in "Heated Kang" is a big problem to rural and urban air pollution. In contrast, the influence of open burning to air quality was limited due to the strict control in harvest season by the local governments. Previous literatures revealed that biomass burning played important role in rural and urban areas of Guanzhong Plain in winter PM pollution (Cao et al., 2005, 2012; Shen et al., 2008, 2009a, 2011b; Zhang et al., 2008b; Okuda et al., 2010; Wang et al., 2014; Zhu et al., 2016). To improve our knowledge on this topic for the Guanzhong Plain, China - an area with large amount of biomass burning, field and laboratory experiments are designed in this study. The objective of the present study are to (1) accurately determine pollutant emission factors (EFs) for major pollutants emitted from local common type of house heating - Chinese 'Heated Kang' straw burning; (2) evaluate the effectiveness of emission control using an advanced type of stove for maize straw pellets burning; and (3) assess the effects of potential regional biomass burning emission reductions on air quality in the Guanzhong Plain.

2. Methodology

2.1. On-site measurements in a residence

The on-site residential maize straw burning experiments were conducted in a house in rural area of Xi'an. In that house, a Chinese 'Heated Kang' and maize straw have been used for heating during the winter. This type of heating in winter has a long history of usage in rural areas in Guanzhong Plain. The fuel used for heating is usually maize straw for maize is the main food crop in this area and maize straw is readily available.

The on-site combustion experiments were conducted at night when the residents usually heat their homes. The maize straw was pre-weighed (~10 kg) before ignition, and a simple air door was adjusted soon after ignition to control the air supply; this led to smoldering conditions, which in turn provided for a long heating time, usually >8 h. The sampling period covered the whole burning cycle (8 h), including flaming combustion (obvious flames) and smoldering phases (without an obvious fire). As a result of the air control provided by the air door, smoldering condition was experienced during most of the sampling period (Fig. S2).

Samples in the residence were collected using a custom-made dilution system with an adjustable dilution rate of 5- to 80-fold. Quartz-fiber filters (Whatman quartz microfiber filters QM/A™) were used to

collect particulate matter in the flue gas using a mini-volume sampler (Airmetrics, Springfield, Oregon, USA), which was operated at a flow rate of 5.0 L·min⁻¹. Size segregated PM samples were collected using an eight-stage cascade impactor (Anderson, Thermo Fisher Scientific, Franklin, MA, USA) with 80 mm diameter quartz membranes at a flow rate of 28.3 L·min⁻¹. The aerodynamic equivalent cut off diameters (D_a, in μm) for each stage were <0.43, 0.43–0.65, 0.65–1.1, 1.1–2.1, 2.1–3.3, 3.3–4.7, 4.7–5.8, and 5.8–9.0, respectively. All filters were pre-combusted at 450 °C for 6 h and equilibrated in a desiccator for 24 h prior to being weighed in preparation for use in the sampler.

2.2. Laboratory simulation

A combustion chamber was set up in a laboratory at the Institute of Earth Environment, Chinese Academy of Sciences (IEECAS) in collaboration with the Desert Research Institute (DRI), USA to simulate the burning of biomass. The combustion chamber was equipped with a thermocouple, a thermo anemometer, an air purification system, and a sampling line connected to a dilution sampler (Wang et al., 2009). An advanced stove was installed in the chamber to simulate residential heating activities. This stove equipped with an automatic fuel feeding system and a secondary air distribution system and was designed for heating function. Maize straw and maize straw pellets burned in the stove respectively. The maize straw pellets were cylindrical and had diameters of 8 mm and random lengths ranging from 5 to 20 mm (Fig. S3). Samples of the combustion emissions were collected with the use of a custom-made dilution system with dilution ratios ranging from 5- to 15-fold. The details of this dilution system have been described in Tian et al. (2015). The sampling periods typically lasted 1–2 h. PM_{2.5} samples were collected on quartz-fiber filters from three parallel channels located downstream of the residence chamber of the dilution sampler with flow rate of 5 L·min⁻¹ per channel. Real-time CO and NO_x (NO and NO₂) levels were monitored by a CO analyzer (Model 48i, Thermo Scientific Inc., Franklin, MA, USA) and a NO_x analyzer (Model 42i, Thermo Scientific Inc., USA) (Wang et al., 2009), respectively. Three non-dispersive infrared (NDIR) CO₂ analyzers (Model SBA-4, PP Systems, Amesbury, MA, USA) were used to measure background CO₂ and CO₂ in the stack and diluted emissions.

2.3. Data analysis

Emission factors (EFs) were calculated by dividing the mass of the emissions by the mass of the fuel consumed, and they are expressed as grams of emission per kilogram of consumed dry fuel (g·kg⁻¹) (Andreae and Merlet 2001). For particulate pollutants including PM_{2.5}, OC, and EC, the EFs were calculated as:

$$EF_p = \frac{m_{\text{filter}} \cdot V_{\text{Total-chimney}}}{Q \cdot m_{\text{fuel}}} \text{DR} \quad (1)$$

where EF_p is the EF for particulate pollutant p for the specific fuel type; m_{filter} is the mass of pollutant collected on the filter; V_{Total-chimney} is the total volume of exhaust flowing through the chimney during the experiment (m³) at standard temperature and pressure; Q is the sampling volume through the filter (m³) at standard temperature and pressure; and m_{fuel} is the mass of the burned fuel. The dilution rate (DR) of the dilution sampler was calculated based on the CO₂ concentrations in different positions, using the following formula:

$$DR = \frac{CO_{2,\text{Stk}} - CO_{2,\text{Bkg}}}{CO_{2,\text{Dil}} - CO_{2,\text{Bkg}}} \quad (2)$$

where CO_{2,Stk} is the CO₂ concentration in stack; CO_{2,Bkg} is the background CO₂ concentration in atmosphere; and CO_{2,Dil} is the CO₂ concentration in the diluted smoke. For gaseous pollutants, including NO_x, CO

and CO₂, the EFs were calculated using online monitored concentrations as follows:

$$EF_p = \frac{V_{\text{Total-chimney}} C_{x,\text{Dilute}}}{m_{\text{fuel}} V_x} M_x DR \quad (3)$$

where $C_{x,\text{Dilute}}$ is the average concentration (molar fraction) measured in the dilution sampler; V_x is the molar-volume of gas at standard temperature and pressure (0.224 m³), and M_x is the molecular weight of species x (g·mol⁻¹) (Ni et al., 2015).

The modified combustion efficiency (MCE) has been used in previous studies to distinguish between flaming and smoldering combustion (Andrae and Merlet, 2001; Oanh et al., 2011; Shen et al., 2011a), and the formula used for calculating the MCE was

$$MCE = \frac{\Delta[\text{CO}_2]}{\Delta[\text{CO}] + \Delta[\text{CO}_2]} \quad (4)$$

where $\Delta[\text{CO}]$ and $\Delta[\text{CO}_2]$ are the excess molar mixing-ratios of CO and CO₂, respectively, that is, the mixing ratio of species “X” in the fire plume minus the corresponding mixing ratio in background air.

Thermal efficiency (TE) is a measure of the ratio of energy delivered to the energy released from fuel complete combustion. And the determination of TE is using the following equation which came from WBT protocol:

$$TE = \frac{E_{\text{H}_2\text{O,heat}} + E_{\text{H}_2\text{O,evap}}}{E_{\text{release}}} \quad (5)$$

where $\Delta E_{\text{H}_2\text{O,heat}}$ is the calorific heat transferred to water from room temperature to boiling point; $\Delta E_{\text{H}_2\text{O,evap}}$ is the calorific heat transferred to water to evaporate; and E_{release} is the total calorific heat released by fuel complete combustion.

A total of 10 types of tests were conducted overall: tests 1–2 involved maize straw smoldering in the Chinese ‘Heated Kang’ at two different burning rates, tests 3–5 focused on the flaming phase of maize straw pellet burning in the advanced stove for ~1 h at three different burning rates, tests 6–8 were for a 1-kg pellet over the whole burning cycle, which lasted ~1 h, at three different burning rates. Maize straw burning with different burning rates were also conducted (Test 9 and 10). However, maize straw was not a proper fuel type for the advanced stove selected in this study due to its bulk in volume and short lasting time in burning cycle (usually 10–15 min in advanced stove condition). Thus tests 9–10 were just for comparison but not a general option for real situation. As straw pellet cannot be fueled in ‘Heated Kang’ due to

its shape and physical feather, this type of test were not conducted in this study. Detailed descriptions for each test are presented in Table 1. The maize straw and maize straw pellets used in this study were analyzed for moisture, volatile matter (VM), ash, fixed carbon, low-heating value (LHV), and high-heating value (HHV) by Analytical Center of the Chinese Academy of Resources, Guangzhou, China. The results of the analyses of these two types of fuels and some other fuels used in previous studies are shown in Table 2.

2.4. PM chemical analysis method

All filter samples collected in this study were kept at –20 °C before being analyzed. First of all, gravimetric analysis of particle mass loadings was determined by a Sartorius MC5 electronic microbalance ($\pm 1 \mu\text{g}$ sensitivity, Sartorius, Göttingen, Germany). One-fourth of each quartz filter sample was used to determine major ion concentrations. Three anions (SO_4^{2-} , NO_3^- and Cl^-) and five cations (Na^+ , NH_4^+ , K^+ , Mg^{2+} , and Ca^{2+}) in aerosol samples were determined by an ion chromatography (IC, Dionex 500, Dionex Corp, Sunnyvale, California, United States). OC and EC in PM₁₀ samples were analyzed using a Thermal and Optical Carbon Analyzer (Model 2001, AtmAA Inc., USA) with IMPROVE (Inter-agency Monitoring of Protected Visual Environment) thermal/optical reflectance (TOR) protocol. The method produced data for four OC fractions (OC1, OC2, OC3, and OC4 in a helium atmosphere at 140 °C, 280 °C, 480 °C, and 580 °C, respectively), a pyrolyzed carbon fraction (OP, determined when reflected laser light attained its original intensity after oxygen was added to the combustion atmosphere), and three EC fractions (EC1, EC2, and EC3 in a 2% oxygen/98% helium atmosphere at 580 °C, 740 °C, and 840 °C, respectively). Detailed operation procedures have been described previously (Shen et al., 2011b).

3. Results and discussion

3.1. Emission factors

The EFs for PM, OC and EC were measured in ten tests under different experimental conditions, and the results are presented in Table 1 along with those for some other fuels that are included for comparison. Large differences were found between the EF_{PMs} for the maize straw and maize straw pellets. That is, the EF_{PMs} for smoldering straw in the ‘Heated Kang’ were $46.14 \pm 1.41 \text{ g}\cdot\text{kg}^{-1}$ for a burning rate of $2 \text{ kg}\cdot\text{h}^{-1}$ and $30.39 \pm 26.48 \text{ g}\cdot\text{kg}^{-1}$ for a burning rate of $1 \text{ kg}\cdot\text{h}^{-1}$ respectively, while the EFs were 23.33 and $11.68 \text{ g}\cdot\text{kg}^{-1}$ when stove was changed to advanced stove with all the other conditions unchanged. These

Table 1
Descriptions, burning conditions and main emission factors of the experiments in this study and cited in previous studies.

Test	Fuel type	Type of stove	MCE, %	Burning rate, kg h ⁻¹	Emission factor, g/kg			Reference
					Particulate matter	Organic carbon (OC)	Elemental carbon (EC)	
1	Maize straw	Heated Kang	–	2	46.1 ± 1.4	17.7 ± 0.74	0.51 ± 0.06	This study (Group I)
2		(smoldering)	–	1	30.4 ± 18.0	11.9 ± 5.0	1.1 ± 0.37	
3	Maize straw pellets	Advanced	92.2 ± 1.3	1	2.3 ± 0.28	0.57 ± 0.12	0.11 ± 0.02	This study (Group II)
4		(flaming only)	94.7 ± 1.2	1.2	3.0 ± 1.1	0.85 ± 0.26	0.31 ± 0.09	
5			95.6 ± 1.2	1.5	3.6 ± 0.76	0.56 ± 0.05	0.55 ± 0.03	This study (Group III)
6	Maize straw pellets	Advanced	86.4 ± 5.1	1	2.5 ± 1.1	1.9 ± 1.3	0.25 ± 0.19	
7		(flaming + smoldering)	91.8 ± 1.6	1.2	4.2 ± 1.0	0.97 ± 0.35	0.13 ± 0.01	
8			92.1 ± 3.4	1.5	5.4 ± 3.5	1.2 ± 0.15	0.18 ± 0.04	This study (Group IV)
9	Maize straw	Advanced	74.5 ± 5.3	2	23.33 ± 8.38	14.04 ± 4.84	0.94 ± 0.12	
10		(flaming + smoldering)	81.6 ± 2.8	1	11.68 ± 0.66	6.66 ± 0.14	0.60 ± 0.02	
	Chinese white poplar	Traditional	94.7 ± 0.9	~3.3	1.80 ± 0.30	0.66 ± 0.32	0.88 ± 0.49	Shen et al., 2012
	Maize straw	Open burning	93.0 ± 2.0	~0.6	12.00 ± 5.40	6.30 ± 3.60	0.28 ± 0.09	Ni et al., 2015
	Bituminous coal	Traditional	–	~1	16.77 ± 2.52	8.29 ± 2.75	3.32 ± 0.55	Chen et al., 2005
	Anthracitic coal	Traditional	–	~1	0.78 ± 0.14	0.039 ± 0.008	0.004 ± 0.000	

Table 2

Moisture, volatile matter (VM), ash, fixed carbon content, high-heating value (HHV) and low-heating value (LHV) for selected fuels.

Fuel types	Moisture, %	Ash, %	VM, %	Fixed carbon, %	HHV, MJ/kg	LHV, MJ/kg	Reference
Maize straw	8.79	3.85	68.93	18.43	14.26	11.39	This study
Maize straw pellets	10.00	3.22	67.11	19.26	16.05	13.09	This study
Chinese white poplar	5.32	0.90	81.69	17.41	18.35	16.22	Shen et al., 2012.
Bituminous coal	–	8.35	37.34	81.93	–	25.27	Chen et al., 2005
Anthracitic coal	–	10.31	8.09	93.17	–	29.65	Chen et al., 2005

results indicated that the advanced stove with secondary air distribution system could reduce EFs of $PM_{2.5} > 50\%$. It was noted that all EF_{PMs} from straw pellets burning in advanced stove were ranging from 2.26 to 5.41 $g \cdot kg^{-1}$, which was roughly one magnitude lower than those from maize straw burning in advanced stove and even more lower than those from “Heated Kang”. Therefore, briquetting of straw could reduce $PM_{2.5}$ emission more effective.

From Table 2, one can see that the composition of the straw and pellets was quite similar, and this implies that there were only minor chemical changes related to the briquetting process. Therefore, the main reasons for the differences in the EFs for the two types of fuels are likely related to variability in the combustion conditions themselves. Furthermore, when compared with other fuels, the VM of the maize straw and pellets were comparable to poplar wood but nearly double the percentage for bituminous coal and even much higher than that for anthracitic coal.

To further investigate the causes for the differences in $PM_{2.5}$ EFs, we compared the combustion conditions and results of the series of experiments are also shown in Table 1. This analysis shows that the largest differences in EF in burning tests were associated with air supply. Maize straw burning in ‘Heated Kang’ is generally limited by the oxygen supply because the residents want to extend the burning time of their stoves for economy and convenience. In contrast, the straw pellets in the advanced stove with secondary air distribution were burned in a relatively oxygen-rich environment and that would tend to enhance the combustion efficiency. Several previous studies had shown that a shortage of oxygen will lead to higher $PM_{2.5}$ EFs (Jenkins et al., 1996; Zhang et al., 2008b; Shen et al., 2012).

Burning rate was another variable that influenced the $PM_{2.5}$ EFs. For the cases involving low-oxygen conditions in the ‘Heated Kang’, the average EF_{pm} for test 1 was ~50% higher than test 2, namely 46.14 and 30.39 $g \cdot kg^{-1}$, and that difference can be explained by the faster burning rate in test 1. Similar results were found in tests 9–10 and also in a previous study by Shen et al. (2012). A possible explanation for the link between the EF_{pm} and burning rate is that faster burning may deplete the oxygen supply thus leading to higher PM emissions as described above.

Another factor that influenced pollutant emissions in our study was the MCE. As an aid in interpreting the results from tests 3–8, the real-time variations in MCE and the gaseous pollutants are plotted together in Fig. 1. From this Fig. 1 and Table 1, it is apparent that lower burning rates usually led to lower MCEs. Furthermore, the MCE had a strong positive correlation with NO , NO_2 and CO_2 emissions; in contrast, CO concentrations had an obvious negative correlation with MCE as also has been reported in prior studies (Shen et al., 2015). Examination of Fig. 1d and e shows that CO had two main peaks, one at the very start of ignition and the other at the end of the burning cycle. Both of these occurred when the MCE was lower than 0.9, a condition that generally regarded as the dividing point between flaming and smoldering combustion. Fig. 1f shows multiple peaks in CO and valleys in CO_2 that were synchronous with decreases in MCE.

Thermal efficiency was the final variable that affected the pollutants’ emission rates (Table 1). Here water-boiling tests (Bailis et al., 2007) were employed to determine the thermal efficiencies for the different burning rates. The test results (Table A.1a) show that test 5 had the highest thermal efficiency and the highest EFs for CO_2 , NO , NO_2 and $PM_{2.5}$ in the flaming pellet studies, and similar results were found in

test 8, the one with the highest thermal efficiency for the pellets studies over a full burning-cycle. In contrast, the lowest EFs for CO were found for test 5 and test 8 for these groups.

Our studies of thermal efficiency show that the characteristics of burning process affect pollutant emissions, and this is important because increasing thermal efficiency would lead to lower fuel usage and that presumably would produce both economic and environmental benefits. To demonstrate this, we converted the units for the EFs from $g \cdot kg^{-1}$ fuel to $g \cdot MJ^{-1}$ (heat transferred), and the results are shown in Table A.1b. In practice, residential heating typically involves semi-continuous burning, and therefore, the results of tests 3 to 5 are likely to be most representative of real conditions. Of these, test 5—the test with the highest thermal efficiency—yielded the lowest EFs for all pollutants. It is important to note that the thermal efficiency of the ‘Heated Kang’ is low, usually $< 10\%$, and our results imply that increasing the thermal efficiency of these stoves could be an effective means for reducing pollutant emissions in China (Qiu et al., 1996).

3.2. Carbonaceous fractions

Numerous studies have shown that the particles emitted from biomass burning are dominated by carbonaceous aerosols, namely OC and EC. Furthermore, the OC/EC ratio can be used to distinguish among combustion sources (Shen et al., 2009b; Ni et al., 2015). The concentrations of the carbonaceous fractions of PM and selected ratios are shown in Table 3. The OC/EC ratios of emissions from straw burning in the Chinese ‘Heated Kang’ were markedly higher than those from pellet burning in the advanced stove. Specifically for test 1, in which the oxygen limitation was severe due to the rapid burning rate and control of the air supply, the OC/EC ratio was as high as 35.1 ± 5.5 , and when the burning rate was reduced by 50% in test 2, the OC/EC ratio decreased to 10.8 ± 1.5 which was at the same level in tests 9 and 10. Both of these values for OC/EC ratios are comparable with those reported in previous studies (Cao et al., 2008; Li et al., 2009). We believe the differences between tests 1(9) and 2(10) are due to effects of the oxygen concentrations on combustion reactions; that is, when oxygen is in short supply, combustion is incomplete, and more unburned and partially-burned organic matter is emitted. This hypothesis could also explain why the gap between tests 9 and 10 was much less than that between tests 1 and 2, which was because tests 9–10 were in relatively oxygen-rich environment.

While the OC/EC ratios from pellet burning were much lower than those from straw burning, OC/EC ratios for tests 3–5 also were obviously lower than for tests 5–8 (as shown in Table 3), and this may reflect the importance of the emissions from the ignition phase. The lower OC/EC ratios compared with the maize straw/Kang results were because the stove used in tests 3–10 had a mechanism for a secondary air supply which burned combustible substances in the smoke produced by the oxygen-deficient combustion. Moreover, a higher temperature in combustor led by secondary air supply could also help to decrease the OC/EC ratio because the formation of EC (Shen et al., 2014). The effect of the secondary air can be seen in the low OC/EC ratio (1.0 ± 0.04) from test 5 which had the highest secondary air supply; the ratio from test 5 was in fact lower than most of those reported for crop residue burning studies (Jenkins et al., 1996; Liouise et al., 1996; Turn et al., 1997; Andreae and Merlet, 2001; Cao et al., 2008).

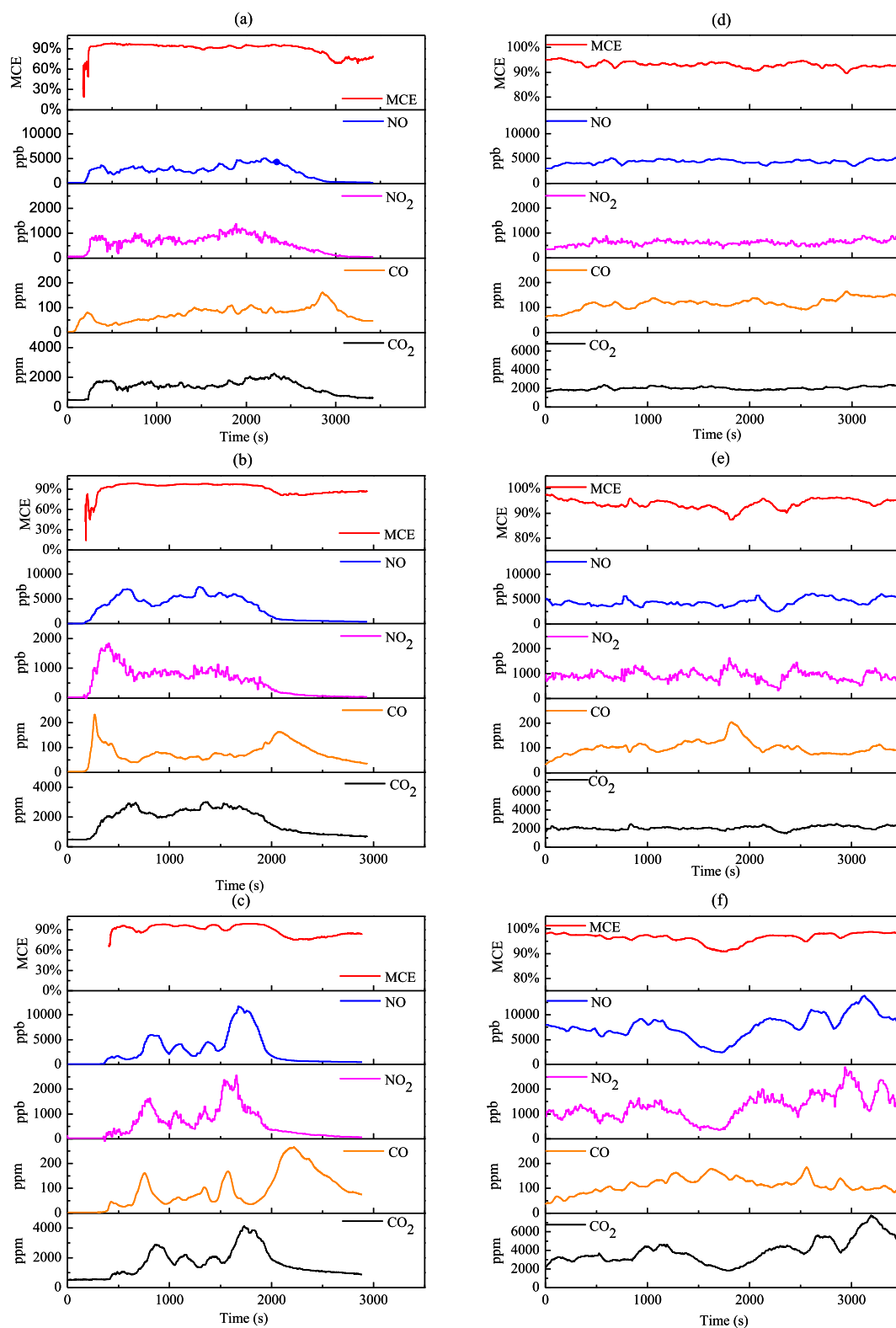


Fig. 1. Time-series plots for modified combustion efficiency (MCE) and PM_{2.5} mass, and NO, NO₂, CO, and CO₂ mixing ratios during residue pellet combustion tests: (a) test 3, (b) test 4, (c) test 5, (d) test 6, (e) test 7, and (f) test 8. Time resolution is 1 s.

Data for seven carbon fractions (OC1, OC2, OC3, OC4, EC1, EC2 and EC3) have been used in source apportionment studies because several important source types have been shown to produce distinctly different abundances of the carbon fractions (Chow et al., 2004; Cao et al., 2005; Cao et al., 2006; Han et al., 2010). As shown in Fig. 2, OC1 and OC2

dominated the carbonaceous fraction in straw burning in “Heated Kang” (Tests 1 and 2), while OC3 and OC4 were the main fractions in the pellet burning studies (Tests 3–8). Fractions OC1 and OC2 are low temperature OC, and the organic matter that composes these two fractions is mostly semi-volatile OC (Chow et al., 2004). The relatively large

Table 3

Emission factors for particulate matter (PM), organic carbon (OC), elemental carbon (EC), and total carbon (TC) and ratios of OC/EC, OC/PM, EC/PM and TC/PM from maize straw and pellet burning.

Test	Stove type and fuel	Burning rate, kg h ⁻¹	Emission factor, g/kg				EF _{OC} /EF _{EC}	EF _{OC} /EF _{PM}	EF _{EC} /EF _{PM}	EF _{TC} /EF _{PM}
			EF _{PM}	EF _{OC}	EF _{EC}	EF _{TC}				
1	Kang-maize straw	2	46.1 ± 1.4	17.7 ± 0.74	0.51 ± 0.06	18.2 ± 0.68	35.1 ± 5.5	0.38 ± 0.01	0.01 ± 0.0	0.39 ± 0.0
2		1	30.4 ± 18.0	11.9 ± 5.0	1.1 ± 0.37	13.0 ± 5.3	10.8 ± 1.5	0.45 ± 0.24	0.04 ± 0.02	0.49 ± 0.26
3	Advanced stove-pellet	1	2.3 ± 0.28	0.57 ± 0.12	0.11 ± 0.02	0.68 ± 0.13	5.4 ± 0.35	0.25 ± 0.02	0.05 ± 0.0	0.30 ± 0.02
4		1.2	3.0 ± 1.1	0.85 ± 0.26	0.31 ± 0.09	1.2 ± 0.35	2.7 ± 0.04	0.29 ± 0.02	0.11 ± 0.01	0.39 ± 0.02
5		1.5	3.6 ± 0.76	0.56 ± 0.05	0.55 ± 0.03	1.1 ± 0.07	1.0 ± 0.04	0.16 ± 0.05	0.16 ± 0.04	0.31 ± 0.08
6	Advanced stove-pellet	1	2.5 ± 1.1	1.9 ± 1.3	0.25 ± 0.19	2.15 ± 1.44	8.3 ± 1.4	0.76 ± 0.18	0.09 ± 0.04	0.83 ± 0.22
7		1.2	4.2 ± 1.0	0.97 ± 0.35	0.13 ± 0.01	1.1 ± 0.35	7.8 ± 3.4	0.25 ± 0.14	0.03 ± 0.0	0.28 ± 0.15
8		1.5	5.4 ± 3.5	1.2 ± 0.15	0.18 ± 0.04	1.4 ± 0.10	6.9 ± 2.2	0.29 ± 0.21	0.04 ± 0.02	0.32 ± 0.23
9	Advanced stove-maize straw	2	23.33 ± 8.38	14.04 ± 4.84	0.94 ± 0.12	18.48 ± 4.98	14.9 ± 3.4	0.60 ± 0.01	0.04 ± 0.01	0.64 ± 0.02
10		1	11.68 ± 0.66	6.66 ± 0.14	0.60 ± 0.02	7.26 ± 0.16	11.1 ± 0.1	0.57 ± 0.02	0.05 ± 0.00	0.62 ± 0.02

fractions of OC1 and OC2 in the straw burning studies were possibly emitted during the smoky, smoldering phase of the experiments when no flames were obvious and the temperatures were relatively low. In contrast, in the pellet burning studies, flaming conditions dominated due to the secondary air supply, and temperatures were higher compared with tests 1 and 2, and more high-temperature OC (OC3 and OC4) was produced. Of these, OC4 has been found to be a mixture of high molecular-weight and polar organic compounds (Grabowsky et al., 2011; Joseph et al., 2012). Pyrolyzed OC (OP) was reported to be associated with water-soluble OC (Yang and Yu, 2002; Ni et al., 2015), and OP was mainly emitted in the smoldering, straw-residue fires. EC was dominated by EC1, which has been proved to be mainly emitted from low temperature burning, e.g. biomass burning (Watson et al., 1994; Han et al., 2007). Very low amounts of EC2 and no EC3 were found in the test samples. For the pellet flaming studies, the sequence of EC1 fractional abundances was test 5 > test 4 > test 3; this indicates that higher temperatures, promoted by more oxygen-rich burning conditions, led to a greater production of EC.

3.3. Water-soluble ions

The EFs for eight water-soluble (WS) ions are shown in Table 4. The total WS ion concentrations composed significant fractions of the PM_{2.5} emitted in both the straw and pellet burning tests. The abundances

ranged from 10% to 36%, and these percentages are consistent with previous studies (Hays et al., 2005; Li et al., 2007; Sillapapiromsuk et al., 2013). Generally, the WS ion contents in PM_{2.5} were lower in the straw smoldering tests (average 13%) compared with the pellet burning ones (average 30%). Previous studies have pointed out that high temperatures produce more EC and WS ions but less OC (McMeeking et al., 2009), and this could explain the low WS ion proportions in tests 1 and 2. Although the relative percentage of WS ions in the pellet burning studies increased, the EFs for each ion decreased by one to two orders-of-magnitude when compared with smoldering straw studies using the 'Heated Kang'.

Potassium ion (K⁺) was the dominant WS cation and chloride (Cl⁻) the dominant WS anion for both the straw and pellet burning sets of tests. The high K⁺ and Cl⁻ emissions were mainly due to the large abundances of these two elements in herbaceous plants (Lindberg et al., 2016). As shown in Table A.3a and A.3b, K⁺ contributed 15–17% and 32–35% of total WS ions for the straw smoldering and pellet burning studies, respectively. In this study, the average percent of K⁺ abundance out of the WS ions in PM_{2.5} was 29%, and that was much higher than the levels in ambient aerosols (3% in normal days and haze days, 4% in dust storm (Shen et al., 2007)). Only during pollution episodes during the straw burning season had the K⁺ percentage of total ions reached 10% (Shen et al., 2009b). This is higher than what would result from coal combustion. Therefore, it can be deduced that K⁺ must be originated

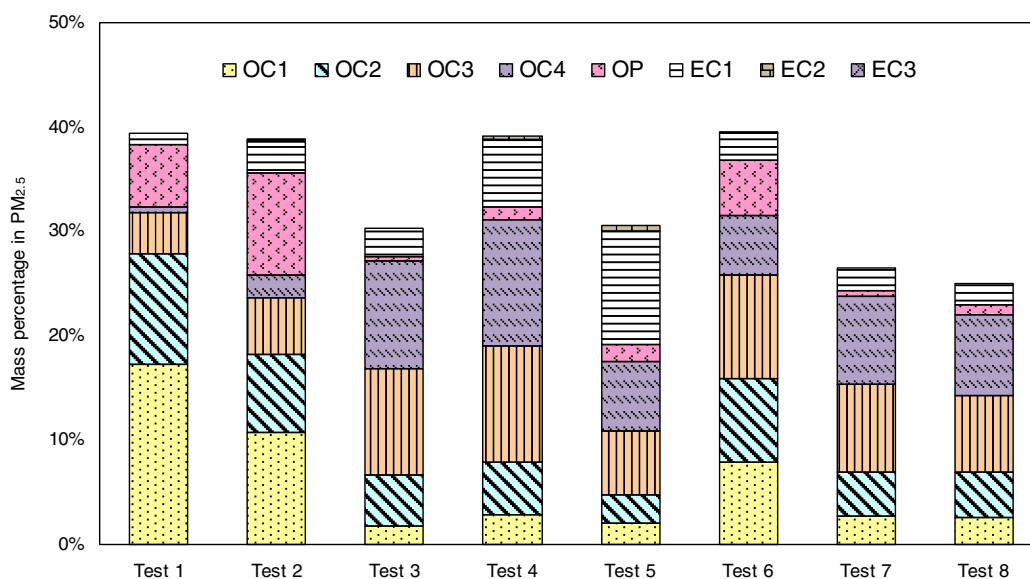


Fig. 2. Mass percentage of thermally resolved organic carbon (OC) and elemental carbon (EC) fractions in PM_{2.5} following IMPROVE_A protocol (Chow et al., 2007). OC1 to OC4 evolve in a 100% helium atmosphere, EC1 to EC3 evolve in a 98% helium/2% oxygen atmosphere. Pyrolyzed OC is the difference between OC and (OC1 + OC2 + OC3 + OC4), and the EC1 values are corrected here by subtracting OP from the original EC1 value.

Table 4
Emission factors for water-soluble ions.

Test	EF _{Na+} mg/kg	EF _{NH4+} mg/kg	EF _{K+} mg/kg	EF _{Mg2+} mg/kg	EF _{Ca2+} mg/kg	EF _{Cl-} mg/kg	EF _{NO3-} mg/kg	EF _{SO42-} mg/kg	∑EF _{ion} g/kg	EF _{PM} g/kg	∑EF _{ion} /EF _{PM} %
1	245.1	201.4	842.4	13.0	228.7	2087.2	323.7	535.7	4.5	46.1	10
2	257.6	206.0	687.8	10.7	175.9	2352.4	470.4	654.5	4.8	30.4	16
3	53.7	83.3	283.1	0.6	3.4	366.7	6.0	24.8	0.8	2.3	36
4	64.3	68.8	350.7	0.7	5.3	492.2	3.8	23.5	1.0	3.0	34
5	74.4	143.0	407.1	0.8	5.5	615.7	5.3	33.9	1.3	3.6	36
6	84.1	58.7	302.7	1.8	23.1	337.4	10.7	37.8	0.9	2.4	35
7	83.4	35.7	319.1	1.9	17.0	263.8	13.2	92.3	0.8	4.1	20
8	91.2	82.0	285.1	2.5	32.6	311.1	12.4	75.4	0.9	5.4	16

primarily from biomass burning. Indeed, K^+ has been used as a marker for biomass burning in aerosol studies for many years (Andreae, 1983).

3.4. Particle size distribution

Fig. 3 shows the mass particle-size distributions of PM emitted from tests 1–5. It is clear that all size distributions from these studies were unimodal and all peaks appeared in particles $<0.47 \mu\text{m}$. The main difference among the tests was that the proportions of submicron particles ($D_a < 1.1 \mu\text{m}$) in the straw burning studies (89% in test 1 and 78% in test 2) were much higher than those from pellet burning (50% in test 3, 63% in test 4 and 70% in test 5). Similar results have been reported for straw residue burning (Shen et al., 2010) and wood burning (Shen et al., 2015). When compared with flaming fires, smoldering fires evidently emitted more fine and ultrafine particles. This also could explain the results of test 5 which had the highest burning rate (1.5 kg h^{-1}) and the smallest average particle size among the three tests in that group. The fast burning rate may have led to a partial oxygen-depletion, which could have led to smoldering-like conditions, and consequently the emission of more fine particles.

The EFs for PM and eight WS ions for different sizes of particles are shown in Fig. 4. Generally, K^+ and Cl^- had the similar variation trends

with the PM mass-size distributions, means they have higher proportions in finer size of particles, which is presumably due to the high concentrations of element K and Cl in the maize straw (Björkman and Strömberg, 1997; Aho and Ferrer, 2005). The EFs for K^+ and Cl^- were the highest of cations and anions, respectively, for the majority of size groups. In contrast, NO_3^- did not exhibit strong relationship with the PM size distribution, and this is likely because NO_3^- concentrations were affected by gas-phase reactions.

For the other ions in Group I and Group II, such as Na^+ , Ca^{2+} and SO_4^{2-} , the levels in PM were generally low but showed higher proportions in the coarse PM compared with fine and ultrafine particles. When compared to other sources of PM, such as coal combustion, vehicle emissions, and fugitive dust, the high percentage of K^+ in fine particles from biomass burning is unique and this is why K^+ had been used a chemical marker for this source for many years (Andreae, 1983; Chow et al., 1993; Shen et al., 2009a).

The OC/EC ratios for different PM size bins were calculated, and the results are shown in Table A.2. For the smoldering straw tests, submicron particles ($D_a < 1.1 \mu\text{m}$) showed slightly higher OC/EC ratios than fine and coarse particles (with p value at 0.01 and 0.05, respectively). The reason is also mainly for smoldering conditions favored the production of ultrafine particles and the smoldering emission had higher OC/EC

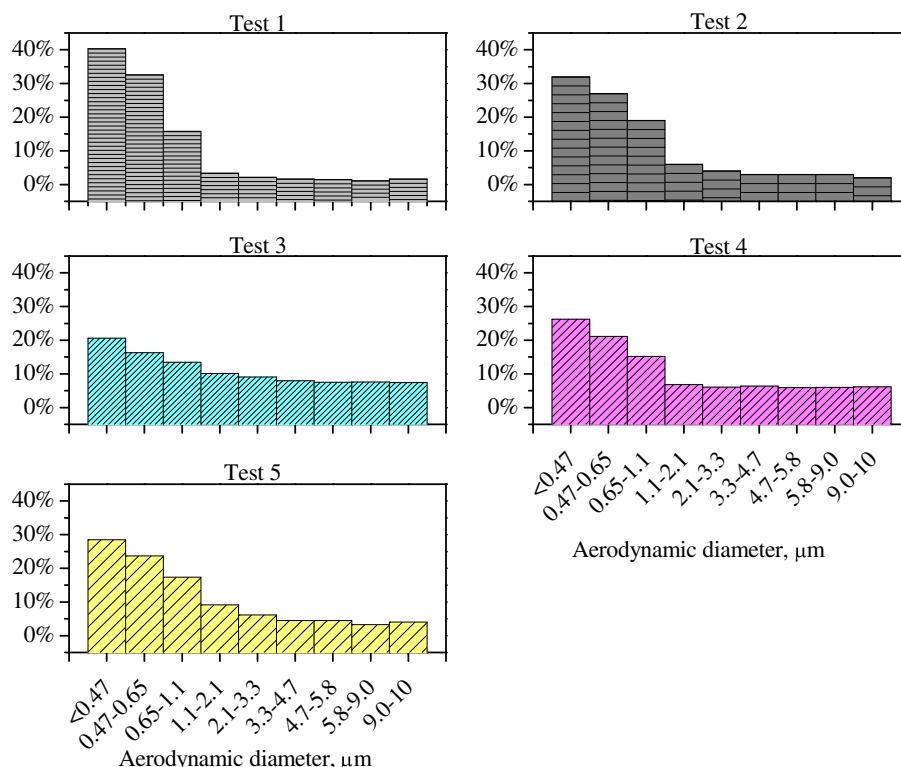


Fig. 3. Size distribution of particulate matter mass from maize straw smoldering (Tests 1 and 2) and residue pellet burning (Tests 3–5).

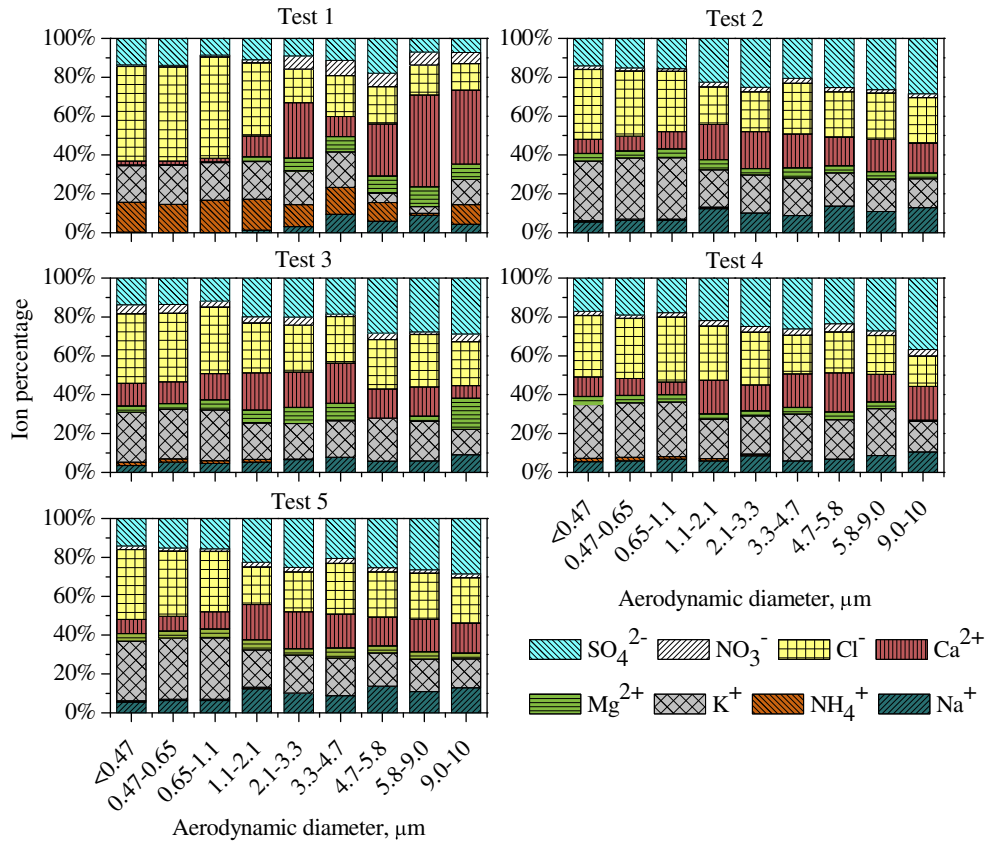


Fig. 4. Water-soluble ion percent abundances in particulate matter from smoldering maize straw (Tests 1 and 2) and maize straw pellets burning (Tests 3–5).

ratios, and that led to the relationship between OC/EC ratios and particle size distributions. Another consequence of these characteristics of the smoldering emissions is that the EF_{OC} also was higher for finer particles. In contrast, for the pellet burning tests, the OC/EC ratios showed a reverse sequence compared with the smoldering straw studies. This was because the high temperatures induced by the secondary air supply burned most of the OC while at the same time producing EC. As noted above, similar results regarding the OC/EC ratios for the pellet studies were found for the carbonaceous fraction of $PM_{2.5}$ (see Fig. 2).

3.5. Evaluation of pollutant emission reduction

Total emissions for the species of interest were estimated as the products of EFs for maize straw and maize straw pellet and the matching usage data (e.g., the amount of maize straw burned for heating). The amount of crop residues burned in Guanzhong Plain was calculated as follows:

$$M = P \times \eta_{harv} \times \eta_{heat} \tag{6}$$

where M is the annual amount of the maize straw burned in Guanzhong Plain in Tg; P is the total annual production of maize straw in Guanzhong Plain in Tg; η_{harv} is the proportion of the maize straw harvested, which was assumed as 70%; and η_{heat} is the proportion of the total harvested maize straw residue used for heating—this was set at 40% as in a previous study (Yan et al., 2006). The total maize straw production (P) in the Guanzhong district was about 5.67 Tg in 2013 according to the Shaanxi Province Statistical Yearbook 2013.

The annual amount of maize straw used for heating (M) was calculated to be 1.59 Tg. The next step was to assume that the residues were used for heating in the following two scenarios: (1) smoldering straw in

‘Heated Kang’ with burning rate of $1 \text{ kg} \cdot \text{h}^{-1}$; (2) pellet burning in advanced stoves with burning rate of $1 \text{ kg} \cdot \text{h}^{-1}$. The results presented in Table 1 show that for Scenario 1 the EF_{PM} was $30.39 \text{ g} \cdot \text{kg}^{-1}$ and for Scenario 2 the EF_{PM} was $2.26 \text{ g} \cdot \text{kg}^{-1}$. For the carbonaceous $PM_{2.5}$ fractions, the EF_{OC} and EF_{EC} for Scenario 1 were $11.92 \text{ g} \cdot \text{kg}^{-1}$ and $1.07 \text{ g} \cdot \text{kg}^{-1}$ respectively, while for Scenario 2 the EF_{OC} was $0.57 \text{ g} \cdot \text{kg}^{-1}$ and the EF_{EC} was $0.11 \text{ g} \cdot \text{kg}^{-1}$.

The annual $PM_{2.5}$ and carbonaceous fractions emissions can be calculated as $Mass_{fuel}$ multiplied by the appropriate EF (Chow et al., 2011). Using this approach for smoldering straw burned in ‘Heated Kang’, the total $PM_{2.5}$ emission was 48.3 Gg, OC emission was 19.0 Gg and EC was 1.7 Gg. For pellet burning in the advanced stove, the total $PM_{2.5}$ emissions was 3.59 Gg, OC was 0.91 Gg, and EC was 0.17 Gg. Comparisons of these values show that the primary $PM_{2.5}$ emissions would be reduced by 92.0% by replacing straw burning in ‘Heated Kang’ with straw pellets in advanced stoves; for OC and EC the reductions would be 95.2% and 90.0%, respectively.

Besides the large reduction in emissions, the atmospheric loadings in the Guanzhong Plain were also calculated using a simplified box model as shown in Fig. 5 (Tie et al., 2015). The east-west dimension of the box was 300 km, the south-north dimension was 100 km, and the height was referenced to the atmospheric boundary layer height, which we assumed to be 300 m on hazy days and 1000 m on non-hazy days. According to the principles of mass conservation, the $PM_{2.5}$ concentrations would be controlled by the surface emissions, secondary PM formation, vertical diffusion, precipitation, and advection. Thus, the $PM_{2.5}$ concentration in the box can be expressed as follows:

$$\frac{\partial[X]}{\partial t} = \frac{\partial[X]_E}{\partial t} + \frac{\partial[X]_T}{\partial t} + \frac{\partial[X]_V}{\partial t} + \frac{\partial[X]_C}{\partial t} + \frac{\partial[X]_D}{\partial t} \tag{7a}$$

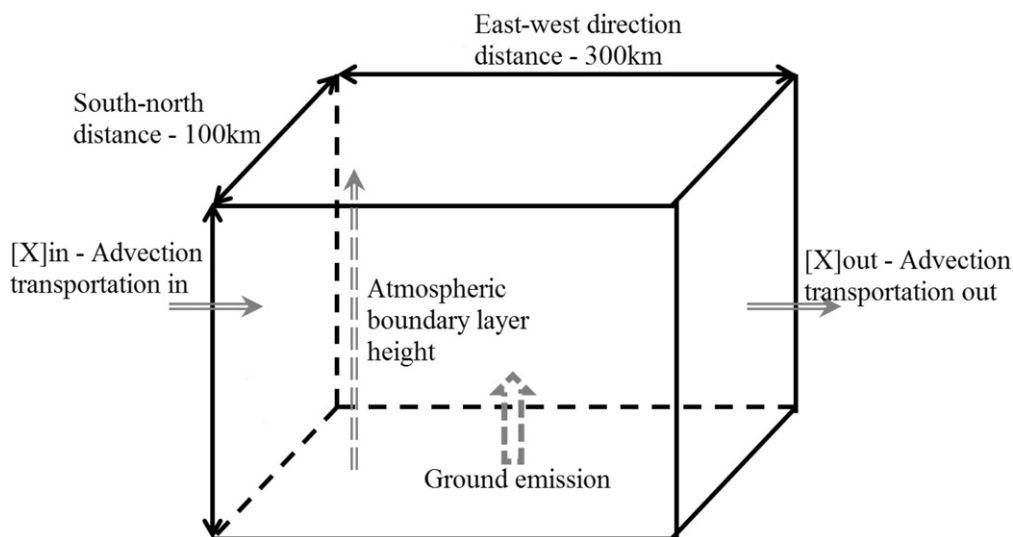


Fig. 5. Features of the box model: east-west distance was 300 km, north-south distance was 100 km, height was equal to that of the atmospheric boundary layer.

where $\frac{\partial[X]}{\partial t}$ is the variation of $\text{PM}_{2.5}$ mass concentration, $[X]_E$ is the $\text{PM}_{2.5}$ surface emission, $[X]_T$ is advective transport, $[X]_V$ is vertical mixing, $[X]_C$ is secondary aerosol formation, and $[X]_D$ is precipitation.

When calculating the atmospheric burden we made the following assumptions: (1) of the secondary inorganic aerosol, which is produced by gas-particle chemical reactions, only NO_x and SO_2 are considered here; thus $[X]_E$ and $[X]_C$ in Eq. (7a) were combined to $[X]_{EC}$; (2) all pollutants emitted into atmosphere were evenly mixed throughout the atmospheric boundary layer; (3) precipitation scavenging of $\text{PM}_{2.5}$ was not considered; (4) pollutant transportation and diffusion were in balance, which meant that $[X]_T = 0$; (5) the heating period is set as 100 days and all fuels were burned evenly throughout the day. Eq. (7a) above was thus simplified to

$$[X]_{t+1} = [X]_t + \frac{[X]_{EC}}{V_{\text{box}}} \times \Delta t \quad (7b)$$

where $[X]_t$ and $[X]_{t+1}$ are the mass concentrations of $\text{PM}_{2.5}$ in $\mu\text{g}\cdot\text{m}^{-3}$ on day t and day $t+1$, the original $\text{PM}_{2.5}$ concentration $[X]_t$ is the average $\text{PM}_{2.5}$ concentration for hazy and non-hazy days minus the contribution from biomass burning. $[X]_{EC}$ is the daily emission of $\text{PM}_{2.5}$, NO_x and SO_2 as shown in Table A.4; V_{box} is the volume of the box, that is, length multiply width and multiply atmospheric boundary layer height (Table A.4); Δt is the time period between t and $t+1$ day. With reference to the $\text{PM}_{2.5}$ concentrations, data from Shen et al. (2009a) indicate that $130.0 \mu\text{g}\cdot\text{m}^{-3}$ is a typical $\text{PM}_{2.5}$ loading for normal days in Xi'an and $350 \mu\text{g}\cdot\text{m}^{-3}$ is more-or-less representative of hazy days. The assumed daily $\text{PM}_{2.5}$ emissions from residue burning contributed 17.1% to the total $\text{PM}_{2.5}$ concentration in the Guanzhong Plain on hazy days and 11.5% on normal days. This result is consistent with the results of previous source apportionment studies in this area (Zhang et al., 2008a; Huang et al., 2014a, b).

The simulated $\text{PM}_{2.5}$ mass concentrations in the Guanzhong Plain after 1 day of heating (Table 5) shows that for non-hazy days, the

straw burned for heating under smoldering conditions contributed $15 \mu\text{g}\cdot\text{m}^{-3}$ to the assumed total $\text{PM}_{2.5}$ loading of $130 \mu\text{g}\cdot\text{m}^{-3}$. For pellets burning, the final $\text{PM}_{2.5}$ mass was $120 \mu\text{g}\cdot\text{m}^{-3}$, and therefore, the simulated emissions were reduced by 7.7%. Under hazy conditions in the model, when the atmospheric boundary layer was shallower, straw burning increased the $\text{PM}_{2.5}$ concentration from $290 \mu\text{g}\cdot\text{m}^{-3}$ to $350 \mu\text{g}\cdot\text{m}^{-3}$ while burning straw pellets in the advanced stove only increased the final $\text{PM}_{2.5}$ concentration to $300 \mu\text{g}\cdot\text{m}^{-3}$, a difference of 14.2%.

The most effective way to solve the pollution emission from biomass burning is replace the straw maize with more clear fuel, such as natural gas or electric power. However, natural gas is not available and electrical power is uneconomical for winter heating in rural areas of Guanzhong Plain. Our results highlighted that replacing traditional straw-burning 'Heated Kang' with advanced stoves that use pellets as fuel may lead to meaningful reductions in pollution emissions and improving the efficiency of energy use in Guanzhong Plain. Moreover, this method can be spread in other undeveloped areas of China to alleviate the air pollution problems after using in rural areas of Guanzhong Plain.

4. Conclusions

The EFs of particles ($\text{PM}_{2.5}$, OC, EC, and water soluble ions) and the particle-size distributions and trace gases (NO_x , CO, and CO_2) from maize straw burning in a traditional 'Heated Kang' and maize straw pellets burning in an advanced stove were determined in this study. The EF_{PM} from straw burning in the 'Heated Kang' was 2–3 times higher than that burning in advanced stove and even ten-times higher than straw pellets burning. The differences in EFs were most likely caused by combustion related parameters, that is, air supply, burning rate, MCE, etc. The OC/EC ratios from residue burning (35.1 and 10.8) were much higher than those from straw pellet burning (range: 1.0 to 8.3), and the ratios were strongly affected by air supply. A test having the highest supply of secondary air ended up with the lowest OC/EC ratio

Table 5
Simulation of $\text{PM}_{2.5}$ mass concentrations from biomass heating emissions.

Fuel type	Conditions	Original $\text{PM}_{2.5}$ concentration, $\mu\text{g}\cdot\text{m}^{-3}$	Final $\text{PM}_{2.5}$ concentration, $\mu\text{g}\cdot\text{m}^{-3}$	Emission reduction efficiency, %	Contribution of biomass burning, %
Maize straw	Non-hazy	115	130	–	11.5
Maize straw pellets	Non-hazy	115	120	7.7	4.2
Maize straw	Hazy	290	350	–	17.1
Maize straw pellets	Hazy	290	300	14.2	3.3

of 1.0. Low temperature OC (OC1 and OC2) dominated the maize-straw burning particles while high temperature OC (OC3 and OC4) were dominant in pellet-burning particles. Low temperature (EC1) was the main EC component in all samples. All particle-size distributions were unimodal, and all peaked in particle sizes $<0.47 \mu\text{m}$. The EFs of K^+ and Cl^- had strong correlations with the EF_{PM} in all sizes of particles due to their high abundances in both the maize straw and pellets while other ions did not show such good correlations, especially in fine particles.

Emission reduction evaluation suggest that replacing straw burning in traditional stoves with pellet burning in advanced stoves could reduce the total $\text{PM}_{2.5}$ emissions from $48.3 \text{ Gg} \cdot \text{year}^{-1}$ to $3.59 \text{ Gg} \cdot \text{year}^{-1}$, a reduction efficiency of 92.0%. A box model simulation also suggests that such a practice could lead to a 7.7% reduction in $\text{PM}_{2.5}$ concentrations (from 130 to $120 \mu\text{g} \cdot \text{m}^{-3}$) in non-hazy conditions and a 14.2% reduction (from 350 to $300 \mu\text{g} \cdot \text{m}^{-3}$) in haze periods. These results suggest that it is possible to effectively reduce $\text{PM}_{2.5}$ emissions from house-hold heating in this region and even other undeveloped areas where there are biomass burning related problems. Additionally, straw pellets could effectively decrease storing space and enhance heating efficiency and its water heating system could isolate smoke from indoor environments when compared with straw heating. Hence, this converting of biomass burning method could help to offer a possible option to mitigate the severe indoor and outdoor air qualities in rural China and other countries facing similar air pollution situations. In future work the performance of straw-pellet and advanced stove in field tests will be conducted to measure the availability of these heating system in residences of Guanzhong Plain. More detail parameters such as temperature and O_2 level in smoke will be measured as well to detect more mechanism of pollution production and emission.

While all the results output from box model were all based on simple assumptions and EF data with high uncertainties, the data should reflect the influence of fuel and stove replacement on $\text{PM}_{2.5}$ emission reduction but not be deemed as accurately quantitative results. Therefore, future work should do more efforts to make this estimation more accurate and reliable.

Acknowledgements

This research was supported by the Natural Science Foundation of Shaanxi Province, China (2016ZDJC-22), National Natural Science Foundation of China (41573101), Chinese Ministry of Science and Technology (2013FY112700), the Fundamental Research Funding for Central Universities in China (xlj2015002), and the Key Lab of Aerosol Chemistry & Physics of the Chinese Academy of Sciences (KLACP201501).

Appendix A. Supplementary data

Supplementary data to this article can be found online at <http://dx.doi.org/10.1016/j.atmosres.2016.10.006>.

References

- Aho, M., Ferrer, E., 2005. Importance of coal ash composition in protecting the boiler against chlorine deposition during combustion of chlorine-rich biomass. *Fuel* 84, 201–212.
- Andreae, M.O., 1983. Soot carbon and excess fine potassium: long-range transport of combustion-derived aerosols. *Science* 220, 1148–1151.
- Andreae, M.O., Merlet, P., 2001. Emission of trace gases and aerosols from biomass burning. *Glob. Biogeochem. Cycles* 15, 955–966.
- Bailis, P.R., Ogle, D., Maccarty, N., From, D.S.I., Smith, K.R., Edwards, R., Energy, H., 2007. *The Water Boiling Test (WBT)*.
- Björkman, E., Strömberg, B., 1997. Release of chlorine from biomass at pyrolysis and gasification conditions. *Energy Fuel* 11, 1026–1032.
- Bond, T.C., Streets, D.G., Yarber, K.F., Nelson, S.M., Woo, J.H., Klimont, Z., 2004. A technology-based global inventory of black and organic carbon emissions from combustion. *J. Geophys. Res. Atmos.* 109, 43.
- Cao, J.J., Wu, F., Chow, J.C., Lee, S.C., Li, Y., Chen, S.W., An, Z.S., Fung, K.K., Watson, J.G., Zhu, C.S., 2005. Characterization and source apportionment of atmospheric organic and elemental carbon during fall and winter of 2003 in Xi'an, China. *Atmos. Chem. Phys.* 5, 3127–3137.
- Cao, J.J., Lee, S.C., Ho, K.F., Fung, K., Chow, J.C., Watson, J.G., 2006. Characterization of roadside fine particulate carbon and its eight fractions in Hong Kong. *Aerosol Air Qual. Res.* 6, 106–122.
- Cao, G.L., Zhang, X.Y., Gong, S.L., Zheng, F.C., 2008. Investigation on emission factors of particulate matter and gaseous pollutants from crop residue burning. *J. Environ. Sci.* 20, 50–55.
- Cao, J.J., Shen, Z.X., Chow, J.C., Watson, J.G., Lee, S.C., Tie, X.X., Ho, K.F., Wang, G.H., Han, Y.M., 2012. Winter and summer $\text{PM}_{2.5}$ chemical compositions in fourteen Chinese cities. *J. Air Waste Manage. Assoc.* 62, 1214–1226.
- Chen, Y.J., Sheng, G.Y., Bi, X.H., Feng, Y.L., Mai, B.X., Fu, J.M., 2005. Emission factors for carbonaceous particles and polycyclic aromatic hydrocarbons from residential coal combustion in China. *Environ. Sci. Technol.* 39, 1861–1867.
- Chow, J.C., Watson, J.G., Lowenthal, D.H., Solomon, P.A., Magliano, K.L., Ziman, S.D., Richards, L.W., 1993. PM_{10} and $\text{PM}_{2.5}$ compositions in California's San Joaquin Valley. *Aerosol Sci. Technol.* 18, 105–128.
- Chow, J.C., Watson, J.G., Kuhns, H., Etyemezian, V., Lowenthal, D.H., Crow, D., Kohl, S.D., Engelbrecht, J.P., Green, M.C., 2004. Source profiles for industrial, mobile, and area sources in the big bend regional aerosol visibility and observational study. *Chemosphere* 54, 185–208.
- Chow, J.C., Watson, J.G., Chen, L.W.A., Chang, M.O., Robinson, N.F., Trimble, D., Kohl, S., 2007. The IMPROVE_A temperature protocol for thermal/optical carbon analysis: maintaining consistency with a long-term database. *J. Air Waste Manage. Assoc.* 9, 1014–1023.
- Chow, J.C., Watson, J.G., Lowenthal, D.H., Chen, L.-W.A., Motallebi, N., 2011. $\text{PM}_{2.5}$ source profiles for black and organic carbon emission inventories. *Atmos. Environ.* 45, 5407–5414.
- Department of Industry and Transport Statistics, National Bureau of Statistics, 2005B. *P.R.C. China Energy Statistical Yearbook 2004*. China Statistics Press, Beijing, China (PRCDIT).
- Grabowsky, J., Streibel, T., Sklorz, M., Chow, J.C., Watson, J.G., Mamakos, A., Zimmermann, R., 2011. Hyphenation of a carbon analyzer to photo-ionization mass spectrometry to unravel the organic composition of particulate matter on a molecular level. *Anal. Bioanal. Chem.* 401, 3153–3164.
- Guenther, A., Karl, T., Harley, P., Wiedinmyer, C., Palmer, P.I., Geron, C., 2006. Estimates of global terrestrial isoprene emissions using MEGAN (model of emissions of gases and aerosols from nature). *Atmos. Chem. Phys.* 6, 3181–3210.
- Gustafsson, O., Krusa, M., Zencak, Z., Sheesley, R.J., Granat, L., Engstrom, E., Praveen, P.S., Rao, P.S.P., Leck, C., Rodhe, H., 2009. Brown clouds over south Asia: biomass or fossil fuel combustion? *Science* 323, 495–498.
- Han, Y.M., Cao, J.J., Chow, J.C., Watson, J.G., An, Z.S., Jin, Z.D., Fung, K.C., Liu, S.X., 2007. Evaluation of the thermal/optical reflectance method for discrimination between char and soot-EC. *Chemosphere* 69, 569–574.
- Han, Y.M., Cao, J.J., Lee, S.C., Ho, K.F., An, Z.S., 2010. Different characteristics of char and soot in the atmosphere and their ratio as an indicator for source identification in Xi'an, China. *Atmos. Chem. Phys.* 10, 595–607.
- Hays, M.D., Fine, P.M., Geron, C.D., Kleeman, M.J., Gullett, B.K., 2005. Open burning of agricultural biomass: physical and chemical properties of particle-phase emissions. *Atmos. Environ.* 39, 6747–6764.
- Huang, Y., Shen, H.Z., Chen, H., Wang, R., Zhang, Y.Y., Su, S., Chen, Y.C., Lin, N., Zhuo, S.J., Zhong, Q.R., Wang, X.L., Liu, J.F., Li, B.G., Liu, W.X., Tao, S., 2014a. Quantification of global primary emissions of $\text{PM}_{2.5}$, PM_{10} , and TSP from combustion and industrial process sources. *Environ. Sci. Technol.* 48 (23), 13834–13843.
- Huang, R.J., Zhang, Y.L., Bozzetti, C., Ho, K.F., Cao, J.J., Han, Y.M., Daellenbach, K.R., Slowik, J.G., Platt, S.M., Canonaco, F., Zotter, P., Wolf, R., Pieber, S.M., Bruns, E.A., Crippa, M., Ciarelli, G., Piazzalunga, A., Schwikowski, M., Abbaszade, G., Schnelle-Kreis, J., Zimmermann, R., An, Z.S., Szidat, S., Baltensperger, U., El Haddad, I., Prevot, A.S.H., 2014b. High secondary aerosol contribution to particulate pollution during haze events in China. *Nature* 514, 218–222.
- Jenkins, B.M., Jones, A.D., Turn, S.Q., Williams, R.B., 1996. Emission factors for polycyclic aromatic hydrocarbons from biomass burning. *Environ. Sci. Technol.* 30, 2462–2469.
- Joseph, A.E., Unnikrishnan, S., Kumar, R., 2012. Chemical characterization and mass closure of fine aerosol for different land use patterns in Mumbai city. *Aerosol Air Qual. Res.* 12, 61–72.
- Latham, T.L., Beyersdorf, A.J., Thornhill, K.L., Winstead, E.L., Cubison, M.J., Hecobian, A., Jimenez, J.L., Weber, R.J., Anderson, B.E., Nenes, A., 2013. Analysis of CCN activity of Arctic aerosol and Canadian biomass burning during summer 2008. *Atmos. Chem. Phys.* 13, 2735–2756.
- Li, X.H., Duan, L., Wang, S.X., Duan, J.C., Guo, X.M., Yi, H.H., Hu, J.N., Li, C., Hao, J.M., 2007. Emission characteristics of particulate matter from rural household biofuel combustion in China. *Energy Fuel* 21, 845–851.
- Li, X.H., Wang, S.X., Duan, L., Hao, J.M., Nie, Y.F., 2009. Carbonaceous aerosol emissions from household biofuel combustion in China. *Environ. Sci. Technol.* 43, 6076–6081.
- Lindberg, D., Niemi, J., Engblom, M., Yrjas, P., Lauren, T., Hupa, M., 2016. Effect of temperature gradient on composition and morphology of synthetic chlorine-containing biomass boiler deposits. *Fuel Process. Technol.* 141, 285–298.
- Liousse, C., Penner, J.E., Chuang, C., Walton, J.J., Eddleman, H., Cachier, H., 1996. A global three-dimensional model study of carbonaceous aerosols. *J. Geophys. Res. Atmos.* 101, 19411–19432.
- McMeeking, G.R., Kreidenweis, S.M., Baker, S., Carrico, C.M., Chow, J.C., Collett, J.L., Hao, W.M., Holden, A.S., Kirchstetter, T.W., Malm, W.C., 2009. Emissions of trace gases and aerosols during the open combustion of biomass in the laboratory. *J. Geophys. Res. Atmos.* 114 (1984–2012).
- Menon, S., Hansen, J., Nazarenko, L., Luo, Y.F., 2002. Climate effects of black carbon aerosols in China and India. *Science* 297, 2250–2253.

- Ministry of Agriculture, 2001. P.R.C. China Agriculture Statistical Report 2000. China Agriculture Press, Beijing, China (PRCMA).
- Ni, H.Y., Han, Y.M., Cao, J.J., Chen, L.W.A., Tian, J., Wang, X.L., Chow, J.C., Watson, J.G., Wang, Q.Y., Wang, P., Li, H., Huang, R.J., 2015. Emission characteristics of carbonaceous particles and trace gases from open burning of crop residues in China. *Atmos. Environ.* 123, 399–406.
- Oanh, N.T.K., Ly, B.T., Tipayarom, D., Manandhar, B.R., Prapat, P., Simpson, C.D., Liu, L.J.S., 2011. Characterization of particulate matter emission from open burning of rice straw. *Atmos. Environ.* 45, 493–502.
- Okuda, T., Okamoto, K., Tanaka, S., Shen, Z.X., Han, Y.M., Huo, Z.Q., 2010. Measurement and source identification of polycyclic aromatic hydrocarbons (PAHs) in the aerosol in Xi'an, China, by using automated column chromatography and applying positive matrix factorization (PMF). *Sci. Total Environ.* 408, 1909–1914.
- Qiu, D.X., Gu, S.H., Catania, P., Huang, K., 1996. Diffusion of improved biomass stoves in China. *Energy Policy* 24 (5), 463–469.
- Rose, D., Nowak, A., Achtert, P., Wiedensohler, A., Hu, M., Shao, M., Zhang, Y., Andreae, M.O., Pöschl, U., 2010. Cloud condensation nuclei in polluted air and biomass burning smoke near the mega-city Guangzhou, China—part 1: size-resolved measurements and implications for the modeling of aerosol particle hygroscopicity and CCN activity. *Atmos. Chem. Phys.* 10, 3365–3383.
- Rosenfeld, D., 1999. TRMM observed first direct evidence of smoke from forest fires inhibiting rainfall. *Geophys. Res. Lett.* 26, 3105–3108.
- Sato, M., Hansen, J., Koch, D., Lacis, A., Ruedy, R., Dubovik, O., Holben, B., Chin, M., Novakov, T., 2003. Global atmospheric black carbon inferred from AERONET. *Proc. Natl. Acad. Sci.* 100, 6319–6324.
- Shen, Z.X., Cao, J.J., Arimoto, R., Zhang, R.J., Jie, D.M., Liu, S.X., Zhu, C.S., 2007. Chemical composition and source characterization of spring aerosol over Horqin sand land in northeastern China. *J. Geophys. Res. Atmos.* 112, D14.
- Shen, Z.X., Arimoto, R., Cao, J.J., Zhang, R.J., Li, X.X., Du, N., Okuda, T., Nakao, S., Tanaka, S., 2008. Seasonal variations and evidence for the effectiveness of pollution controls on water-soluble inorganic species in total suspended particulates and fine particulate matter from Xi'an, China. *J. Air Waste Manage. Assoc.* 58, 1560–1570.
- Shen, Z.X., Cao, J.J., Arimoto, R., Han, Z.V., Zhang, R.J., Han, Y.M., Liu, S.X., Okuda, T., Nakao, S., Tanaka, S., 2009a. Ionic composition of TSP and PM_{2.5} during dust storms and air pollution episodes at Xi'an, China. *Atmos. Environ.* 43, 2911–2918.
- Shen, Z.X., Cao, J.J., Tong, Z., Liu, S.X., Reddy, L.S.S., Han, Y.M., Zhang, T., Zhou, J., 2009b. Chemical characteristics of submicron particles in winter in Xi'an. *Aerosol Air Qual. Res.* 9, 80–93.
- Shen, G.F., Yang, Y.F., Wang, W., Tao, S., Zhu, C., Min, Y.J., Xue, M.A., Ding, J.N., Wang, B., Wang, R., Shen, H.Z., Li, W., Wang, X.L., Russell, A.G., 2010. Emission factors of particulate matter and elemental carbon for crop residues and coals burned in typical household stoves in China. *Environ. Sci. Technol.* 44, 7157–7162.
- Shen, G.F., Wang, W., Yang, Y.F., Ding, J.N., Xue, M.A., Min, Y.J., Zhu, C., Shen, H.Z., Li, W., Wang, B., Wang, R., Wang, L., Tao, S., Russell, A.G., 2011a. Emissions of PAHs from indoor crop residue burning in a typical rural stove: emission factors, size distributions, and gas-particle partitioning. *Environ. Sci. Technol.* 45, 1206–1212.
- Shen, Z.X., Cao, J.J., Liu, S.X., Zhu, C.S., Wang, X., Zhang, T., Xu, H.M., Hu, T.F., 2011b. Chemical composition of PM₁₀ and PM_{2.5} collected at ground level and 100 meters during a strong winter-time pollution episode in Xi'an, China. *J. Air Waste Manage. Assoc.* 61, 1150–1159.
- Shen, G.F., Wei, S.Y., Wei, W., Zhang, Y.Y., Min, Y.J., Wang, B., Wang, R., Li, W., Shen, H.Z., Huang, Y., Yang, Y.F., Wang, W., Wang, X.L., Wang, X.J., Tao, S., 2012. Emission factors, size distributions, and emission inventories of carbonaceous particulate matter from residential wood combustion in rural China. *Environ. Sci. Technol.* 46, 4207–4214.
- Shen, G.F., Xue, M., Chen, Y.C., Yang, C.L., Li, W., Shen, H.Z., Huang, Y., Zhang, Y.Y., Chen, H., Zhu, Y., Wu, H., Ding, A.J., Tao, S., 2014. Comparison of carbonaceous particulate matter emission factors among different solid fuels burned in residential stoves. *Atmos. Environ.* 89 (33), 7e345.
- Shen, G.F., Chen, Y.C., Xue, C.Y., Lin, N., Huang, Y., Shen, H.Z., Wang, Y.L., Li, T.C., Zhang, Y.Y., Su, S., Huangfu, Y.B., Zhang, W.H., Chen, X.F., Liu, G.Q., Liu, W.X., Wang, X.L., Wong, M.H., Tao, S., 2015. Pollutant emissions from improved coal- and wood-fuelled cookstoves in rural households. *Environ. Sci. Technol.* 49, 6590–6598.
- Sillapapiromsuk, S., Chantara, S., Tengjaroenkul, U., Prasitwattanaseree, S., Prapamontol, T., 2013. Determination of PM₁₀ and its ion composition emitted from biomass burning in the chamber for estimation of open burning emissions. *Chemosphere* 93, 1912–1919.
- Streets, D.G., Bond, T.C., Carmichael, G.R., Fernandes, S.D., Fu, Q., He, D., Klimont, Z., Nelson, S.M., Tsai, N.Y., Wang, M.Q., Woo, J.H., Yarber, K.F., 2003. An inventory of gaseous and primary aerosol emissions in Asia in the year 2000. *J. Geophys. Res. Atmos.* 108, 23.
- Tian, J., Chow, J.C., Cao, J.J., Han, Y., Ni, H.Y., Chen, L.W.A., Wang, X.L., Huang, R.J., Moosmuller, H., Watson, J.G., 2015. A biomass combustion chamber: design, evaluation, and a case study of wheat straw combustion emission tests. *Aerosol Air Qual. Res.* 15, 2104–2114.
- Tie, X.X., Zhang, Q., He, H., Cao, J.J., Han, S.Q., Gao, Y., Li, X., Jia, X.C., 2015. A budget analysis of the formation of haze in Beijing. *Atmos. Environ.* 100, 25–36.
- Turn, S.Q., Jenkins, B.M., Chow, J.C., Pritchett, L.C., Campbell, D., Cahill, T., Whalen, S.A., 1997. Elemental characterization of particulate matter emitted from biomass burning: Wind tunnel derived source profiles for herbaceous and wood fuels. *J. Geophys. Res. Atmos.* 102, 3683–3699.
- Wang, X.L., Chancellor, G., Evenstad, J., Farnsworth, J.E., Hase, A., Olson, G.M., Sreenath, A., Agarwal, J.K., 2009. A novel optical instrument for estimating size segregated aerosol mass concentration in real time. *Aerosol Sci. Technol.* 43, 939–950.
- Wang, D.X., Hu, J.L., Xu, Y., Lv, D., Xie, X.Y., Kleeman, M., Xing, J., Zhang, H.L., Ying, Q., 2014. Source contributions to primary and secondary inorganic particulate matter during a severe wintertime PM_{2.5} pollution episode in Xi'an, China. *Atmos. Environ.* 97, 182–194.
- Wang, L., Xin, J., Li, X., Wang, Y., 2015. The variability of biomass burning and its influence on regional aerosol properties during the wheat harvest season in North China. *Atmos. Res.* 157, 153–163.
- Watson, J.G., Chow, J.C., Lowenthal, D.H., Pritchett, L.C., Frazier, C.A., Neuroth, G.R., Robbins, R., 1994. Differences in the carbon composition of source profiles for diesel- and gasoline-powered vehicles. *Atmos. Environ.* 28, 2493–2505.
- Yan, X.Y., Ohara, T., Akimoto, H., 2006. Bottom-up estimate of biomass burning in mainland China. *Atmos. Res.* 40, 5262–5273.
- Yang, H., Yu, J.Z., 2002. Uncertainties in charring correction in the analysis of elemental and organic carbon in atmospheric particles by thermal/optical methods. *Environ. Sci. Technol.* 36, 5199–5204.
- Zhang, T., Claeys, M., Cachier, H., Dong, S.P., Wang, W., Maenhaut, W., Liu, X.D., 2008a. Identification and estimation of the biomass burning contribution to Beijing aerosol using levoglucosan as a molecular marker. *Atmos. Environ.* 42, 7013–7021.
- Zhang, Y.X., Dou, H., Chang, B., Wei, Z.C., Qiu, W.X., Liu, S.Z., Liu, W.X., Tao, S., 2008b. Emission of polycyclic aromatic hydrocarbons from indoor straw burning and emission inventory updating in China. In: Carpenter, D.O. (Ed.), *Environmental Challenges in the Pacific Basin*. Wiley-Blackwell, Malden, pp. 218–227.
- Zhang, H.F., Hu, D.W., Chen, J.M., Ye, X.N., Wang, S.X., Hao, J.M., Wang, L., Zhang, R.Y., An, Z.S., 2011. Particle size distribution and polycyclic aromatic hydrocarbons emissions from agricultural crop residue burning. *Environ. Sci. Technol.* 45, 5477–5482.
- Zhang, Q., Shen, Z.X., Cao, J.J., Zhang, R.J., Zhang, L.M., Huang, R.J., Zheng, C.J., Wang, L.Q., Liu, S.X., Xu, H.M., Zheng, C.L., Liu, P.P., 2015. Variations in PM_{2.5}, TSP, BC, and trace gases (NO₂, SO₂, and O₃) between haze and non-haze episodes in winter over Xi'an, China. *Atmos. Environ.* 112, 64–71.
- Zhu, C.S., Cao, J.J., Tsai, C.J., Shen, Z.X., Liu, S.X., Huang, R.J., Zhang, N.N., Wang, P., 2016. The rural carbonaceous aerosols in coarse, fine, and ultrafine particles during haze pollution in northwestern China. *Environ. Sci. Pollut. Res.* 23, 4569–4575.